Available online at www.sciencedirect.com
SCIENCE DIRECT
ELSEVIER
Journal of the European Ceramic Society 26 (2006) 2319–2326
ECERS
www.elsevier.com/locate/jeurceramsoc

Nanocrystalline $BaTiO_3$ powder via a sol process ambient conditions

Xinyu Wang [a], Burtrand I. Lee [a,*], Michael Hu [b], E. Andrew Payzant [b], Douglas A. Blom [b]

[a] *School of Materials Science and Engineering, Clemson University, SC 29634, USA*
[b] *Oak Ridge National Laboratory, Oak Ridge, TN 37831, USA*

Received 30 June 2004; received in revised form 28 March 2005; accepted 9 April 2005
Available online 23 May 2005

Abstract

Nanocrystalline $BaTiO_3$ particles have been prepared by ambient condition sol (ACS) process starting from soluble precursors of barium and titanium yielding a mixed oxide/hydroxide gel. The gel was peptized and crystallized in water under a refluxing condition. Higher initial pH and Ba/Ti ratio led to smaller crystallite sizes of $BaTiO_3$ powders. Organic mineralizer, tetramethylammonium hydroxide (TMAH), can adsorb on the $BaTiO_3$ nuclei and inhibited further growth of the particles. Adding a polymer during $BaTiO_3$ synthesis led to a smaller particle size and increased redispersibility of the particles in water.

Keywords: Sol–gel processes; Powder-chemical preparation; $BaTiO_3$; Titanates

1. Introduction

Because of the wide applications of barium titanate ($BaTiO_3$) in such parts as multilayer ceramic capacitors (MLCC), transducers, positive temperature coefficient of resistance (PTCR) thermistors, etc., based on the excellent dielectric and ferroelectric properties, there are enormous quantity of literature on the preparation of this material.[1–11] Most of these preparation of $BaTiO_3$ involve high temperatures and/or pressures. Traditionally, $BaTiO_3$ is prepared by solid-state reaction of fine barium carbonate ($BaCO_3$) and titanium dioxide (TiO_2) powders at high temperatures above 1000 °C followed by milling.[12–15]

The MLCC industry is continuing intensive efforts to reduce component size with increasing the volumetric efficiency of the MLCCs by decreasing the dielectric layer thickness down to 1–2 μm.[16] In the past decades, extensive studies have been conducted to produce nanosized $BaTiO_3$ powders with narrow particle size distribution, controlled morphology, and high purity. $BaTiO_3$ nanocrystals have been synthesized by various techniques: hydrothermal method,[7,17–35] sol–gel process,[36–41] low temperature aqueous synthesis (LTAS),[42–44] low temperature direct synthesis (LTDS),[45,46] combustion synthesis[47], oxalate coprecipitation route,[2,48] microwave heating,[49] and microemulsion process.[50]

Hennings et al.[19] synthesized $BaTiO_3$ powders from Ba/Ti acetate gel precursors by a two-step route: transparent gels of Ba/Ti acetate was formed by sol–gel process followed by hydrothermal treatment. Thermaogravimetric analysis (TGA) and titration results revealed stoichiometric composition of Ba/Ti gels. They also observed by transmission electron microscopy (TEM) that nucleation began after 30 min: large number of tiny (<5 nm) $BaTiO_3$ nuclei formed on the surface of the gel. The reaction completed after 10 h and 200–300 nm $BaTiO_3$ particles were produced.

As for the morphology control, Lu et al.[31] reported synthesizing $BaTiO_3$ by hydrothermal method in the presence of Tween 80 as a surface modifier. Ultrafine (<100 nm) $BaTiO_3$ particles with narrow size distribution were obtained. Those powders also showed good redispersibility. Hu and coworkers[33] produced $BaTiO_3$

* Corresponding author. Tel.: +1 864 6565348; fax: +1 864 5651453.
E-mail address: burt.lee@ces.clemson.edu (B.I. Lee).

0955-2219/$ – see front matter © 2005 Elsevier Ltd. All rights reserved.
doi:10.1016/j.jeurceramsoc.2005.04.002

powders in a two-stage hydrothermal approach, which involves dielectric tuning solution (DTS) precipitation of TiO_2 spheres in a mixed solvent system of isopropanol and water. Wada and coworkers[45,46] established LTDS method to synthesize nanosize $BaTiO_3$ powders using highly concentrated aqueous solution of $Ba(OH)_2$. They proposed that the heat of neutralization between strong acid and base could be used to drive the formation of $BaTiO_3$ crystals directly from Ba and Ti ions, via no intermediates. For the first time, $BaTiO_3$ particles with crystallite size less than 10 nm was reported. However, hydroxyl group was detected as an impurity and the Ba/Ti ratio was 0.786 ± 0.005, indicating the presence of many Ba vacancies in the crystallies.

Since water is the common medium in the hydrothermal, LTAS and LTDS, it's inevitable to incorporate much OH species into $BaTiO_3$ lattice as defects.[51] Hennings and coworkers[19,20,27] characterized hydrothermal $BaTiO_3$ powders and found OH groups were incorporated in the perovskite lattice. A defect chemical model was derived and the lattice defects were calculated from TGA data. It is well known that such defects can lead to deviation of stoichiometry, poor sintering density, and inhomogeneous microstrucure of green tapes.[19] Thus, reducing such kind of defects is a challenge in $BaTiO_3$ synthesis.

The newly developed solvothermal method, which involves an organic solvent instead of water,[52,53] may provide an alternative to producing defects free $BaTiO_3$ nanoparticles. In the work of Chen and Jiao,[53] Ba and Ti alkoxides were mixed in $HOCH_2CH_2OCH_3$ and hydrolyzed to form precursor gel. The gel was dried under vacuum and the dried xerogel was solvothermally treated in alcohol at 140–240 °C for up to 144 h. Cubic $BaTiO_3$ particles with small particle size of 20–60 nm and narrow particle size distribution were obtained. It was observed that solvothermal reaction was much slower than hydrothermal, attributing to the low solubility of precursor gel in alcohol. However, no defect analysis was reported in their paper.

O'Brien et al.[54] developed "injection-hydrolysis" procedure to produce high purity, crystalline nanoscale materials using barium titanium ethyl hexano-isopropoxide. In the mixture with diphenylether and oleic acid at 140 °C under argon, hydrogen peroxide was injected and the sol to promote further hydrolysis and crystallization. Monodisperse nanoparticles of $BaTiO_3$ with diameters ranging from 6 to 12 nm were obtained. However, no defect analysis was carried out in their research. Moreover, since hydrogen peroxide was used, existence of lattice hydroxyl groups is expected.

In our previous publications,[55,56] we reported the superior features of this synthetic method; ambient condition sol (ACS) process producing nanocrystalline $BaTiO_3$ powders, to other reported processing techniques. In this paper, we present more details of the effect of experimental variables on the morphology and properties $BaTiO_3$ particles under the definition of an ambient condition as a near room temperature and pressure.

Table 1
List of $BaTiO_3$ samples prepared by the ACS process

Sample ID	Ba/Ti	Mineralizer	pH	Reaction time (h)	Medium
BT1	1.5:1	KOH	12.0	20	H_2O
BT2	1.5:1	KOH	14.0	20	H_2O
BT3	1.5:1	KOH	14.2	20	H_2O
BT4	1.5:1	KOH	14.0	6	H_2O
BT5	3:1	KOH	14.0	20	H_2O
BT6	1.5:1	KOH	14.0	20	H_2O
BT7	1.5:1	KOH	14.0	20	H_2O
BT8	1.5:1	TMAH	14.0	20	H_2O
BT9	1.5:1	KOH	14.0	20	H_2O

BT1-5 and 8: $BaCl_2 + TiCl_4$ precursors; BT6: $Ti(OC_2H_5)_4$ as Ti source; BT7: $Ba(OOCCH_3)_2$ as Ba source; BT8: With 2 mg APA per ml.

2. Experimental

All the chemical reagents used in this research were analytical grade and no further purification was performed before use. The experimental procedure was described in our previous work.[55,56] To study the influence of experimental parameters on the properties of final $BaTiO_3$ products, a series of $BaTiO_3$ samples have been prepared as described in Table 1.

Dynamic light scattering (DLS, Model BI-9000AT, Brookhaven Instruments Corp., Holtsville, NY) was applied to estimate the particle size and particle size distribution of resulting $BaTiO_3$ powders after ultrasonicated for 15 min.

Room temperature X-ray diffraction (RTXRD, Scintag PAD V using Cu Kα with $\lambda = 0.15406$ nm) was used for crystalline phase identification and determination of crystallite size of the powder. The crystallite size of $BaTiO_3$ powders was calculated by the Scherrer equation:

$$d_x = \frac{0.94\lambda}{\beta\cos\theta} \quad (1)$$

where d_x is the crystallite size, λ is the X-ray wavelength, β is the full-width at half-maximum (FWHM), and θ is the diffraction angle. The (2 0 0) peak was used to calculate the crystallite size.

The morphology of $BaTiO_3$ powders was examined by scanning electron microscopy (SEM) and transmission electron microscopy (TEM). A small amount of $BaTiO_3$ particles was deposited on a carbon tape attached to the brass stub, then air spray was applied to blow off the excess $BaTiO_3$ powders. The $BaTiO_3$ powders were then coated with gold via plasma sputtering (Hammer 6.2 Sputtering System, Anatech). To prepare TEM samples, a tiny amount of $BaTiO_3$ particles was dispersed into isopropanol by grinding in an agate mortar. A copper grid with a supported thin carbon film was dipped into the suspension, removed and dried on a filter paper.

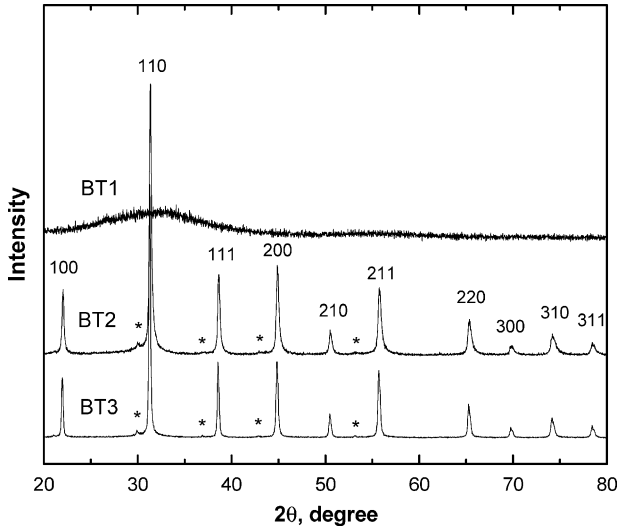

Fig. 1. RTXRD patterns of $BaTiO_3$ samples prepared at pH 12 (BT1), 14 (BT2) and 14.2 (BT3). '*' These are fluorescence signals originating from the copper anti-cathode of tungsten filament in the XRD instrument.

3. Results and discussions

3.1. Effect of solution pH

To study the impact of the solution pH on particle morphology and crystal structure, $BaTiO_3$ gels were formed at pH 12, 14 and 14.2 for BT1, BT2, and BT3, respectively. The RTXRD patterns in Fig. 1 indicate that $BaTiO_3$ powders prepared at pH 12 (BT1) is amorphous, while the $BaTiO_3$ powders prepared above pH 14 (BT2 and BT3) are well crystallized cubic phase. It can be concluded that the alkalinity plays an important role in the crystallization of $BaTiO_3$ in the ACS process. According to the thermodynamic model[57] for the hydrothermal process, phase-pure $BaTiO_3$ could only be obtained at a pH higher than 13.5.

The diffraction peaks of BT3 from pH 14.2 are slightly broader than BT2 from pH 14.0, indicating a smaller crystallite size of BT3. Calculated from the FWHM of (2 0 0) peak using Eq. (1), the crystallite size of BT3 is indeed smaller with 42.6 ± 1.8 nm than that of BT2 with 51.5 ± 1.5 nm as given in Table 2. At a higher pH, a greater supersaturation by the increased solubility of the precursor gel leading to greater nucleation rate than the growth rate.[22]

Fig. 2 shows the micrographs of $BaTiO_3$ powders synthesized under different pHs and Ba/Ti ratios. No individual particles could be seen in the chalky mass of BT1 sample gelled at pH 12 (Fig. 2a), which agrees with the RTXRD pattern in Fig. 1. BT2 particles formed at pH 14 are spherical with slight agglomeration and narrow particle size distribution. The DLS results in Table 2 show that the mean particle size is 126 ± 15 nm. Comparing with BT2 formed at pH 14, BT3 particles formed at pH 14.2 are more agglomerated with smaller particle size of 91 ± 18 nm.

The above results show that a higher pH of reaction media leads to smaller particle size of $BaTiO_3$ for the reasons given above for the crystallite size.

3.2. Effect of refluxing time

BT4 was prepared at pH 14.0 with Ba/Ti = 1.5 in an aqueous medium for 6 h. The RTXRD pattern in Fig. 3 reveals well-crystallized cubic phase. The crystallite size of BT4 calculated from FWHM of (2 0 0) peak by Eq. (1) is 50 ± 2 nm, which is statistically same as that of BT2. The DLS and SEM results indicate that the morphology and particle size of BT4 (112 ± 20) are similar to that of BT2 (126 ± 15) which was prepared under the same condition but for a longer time of 20 h. Our previous study[56] showed that the formation of $BaTiO_3$ nanoparticles followed an "in situ transformation" mechanism and was a rapid process (within 30 min). Once the crystal particles are formed, extending the reaction time on the morphology, particle size, crystallite size, and crystallinity of $BaTiO_3$ particles has little or no effect.

3.3. Effect of the initial Ba/Ti ratio

To study the influence of Ba/Ti ratio in the starting materials under the same pH, reaction temperature, and time, $BaTiO_3$ powders was prepared with initial Ba/Ti = 3:1 (BT5). No splitting of (2 0 0) peak at $2\theta = 44.95^\circ$ is found in RTXRD pattern (Fig. 4), indicative of cubic phase structure with symmetry Pm3m. Calculating from the FWHM of (2 0 0) peak by Scherrer's formula of Eq. (1), the crystallize size of BT5 sample is 41.9 ± 1.6 nm, slightly smaller than that of BT2 from Ba/Ti = 1.5.

As shown in Fig. 2d, the morphology of BT5 powders is somewhat finer. Comparing with BT2 powders (Ba/Ti = 1.5), noticeably smaller particles with smaller particle-size distribution is found in BT5 sample (Ba/Ti = 3). One can also notice the increased degree of agglomeration of BT5 particles. The DLS results show that the mean particle size of BT5 is 79 ± 10 nm. Similar observation was reported by Wada et al. [45] for $BaTiO_3$ powders prepared by LTDS method, at a fixed reaction temperature, increasing Ba/Ti ratio resulted in smaller crystallite size (37.0 nm when

Table 2
Crystallite size and particle size of ACS $BaTiO_3$ powders

	BT2	BT3	BT4	BT5	BT6	BT7	BT8	BT9
Crystallite size (nm)	52 ± 2	43 ± 2	50 ± 2	42 ± 2	50 ± 2	53 ± 2	<10	47 ± 1
Particle size (nm)	126 ± 15	91 ± 18	112 ± 20	79 ± 10	207 ± 23	164 ± 38	146 ± 16	82 ± 13

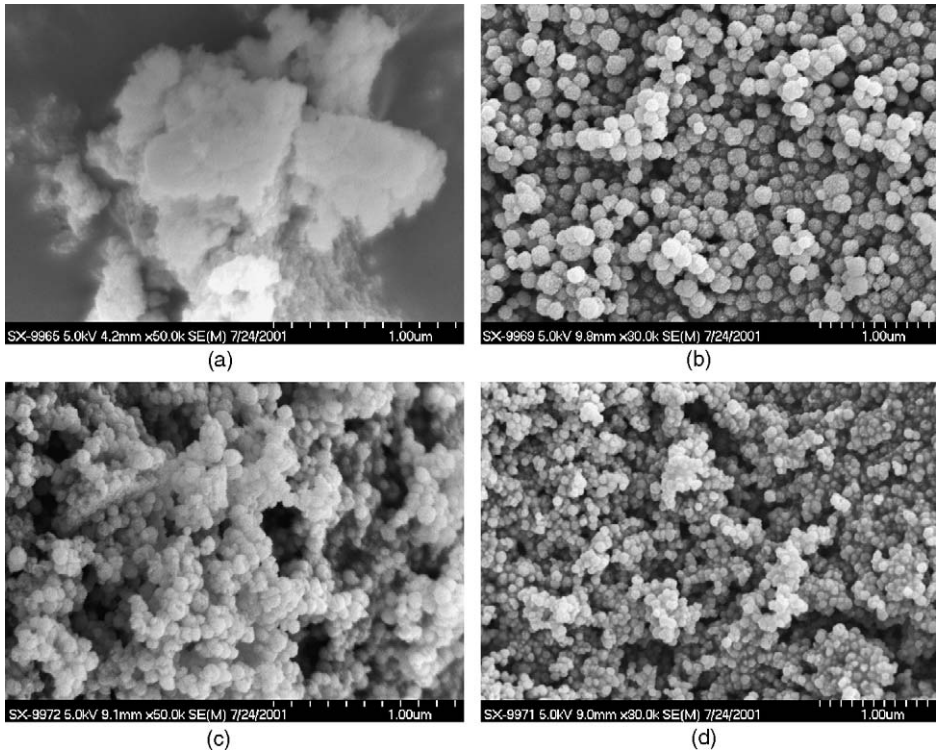

Fig. 2. SEM micrographs of $BaTiO_3$ powders, (a) BT1 (pH 12, Ba/Ti = 1.5); (b) BT2 (pH 14, Ba/Ti = 1.5); (c) BT3 (pH 14.2, Ba/Ti = 1.5); (d) BT5 (pH 14, Ba/Ti = 3).

Ba/Ti = 5 and 12.9 nm when Ba/Ti > 35). The Ba/Ti ratios of the final product powders determined by inductively coupled plasma spectroscopy were varied by the starting Ba/Ti ratios. The starting ratios of 1 and 2 yielded Ba/Ti ratios of 0.89 and 1.01 in the final product powders. The detailed results and discussion are reported in a separate publication.[59]

3.4. Influence of anions

To study the influence of the anions of the metallic precursors on the morphology of ACS $BaTiO_3$, two different $BaTiO_3$ samples were prepared. BT6 was prepared from $Ti(OC_2H_5)_4$ and $BaCl_2$, while BT7 was synthesized from $TiCl_4$ and $Ba(OOCCH_3)_2$ (Table 1). All the experimental

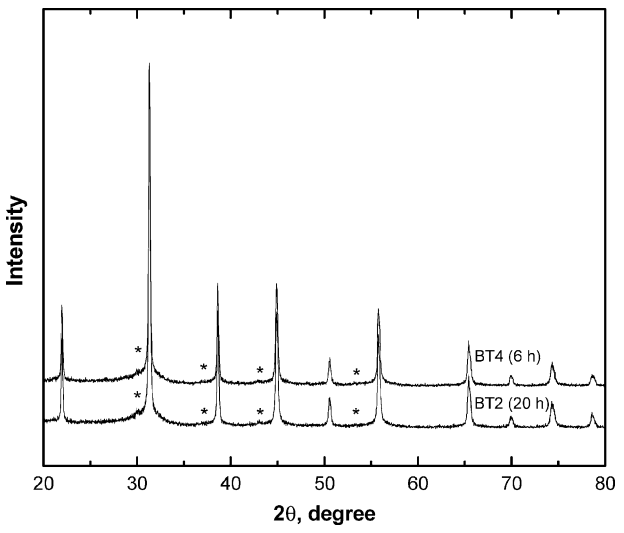

Fig. 3. RTXRD patterns of $BaTiO_3$ powders prepared with different reaction time. '*' These are fluorescence signals originating from the copper anti-cathode of tungsten filament in the XRD instrument.

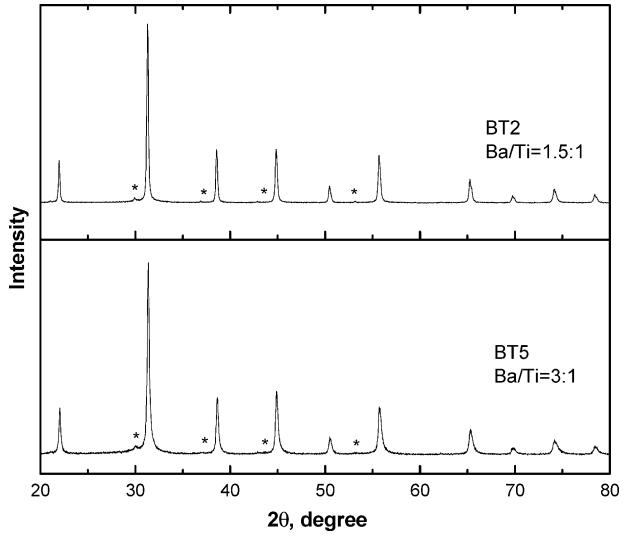

Fig. 4. RTXRD patterns of $BaTiO_3$ powders prepared with different initial Ba/Ti ratio. '*' These are fluorescence signals originating from the copper anti-cathode of tungsten filament in the XRD instrument.

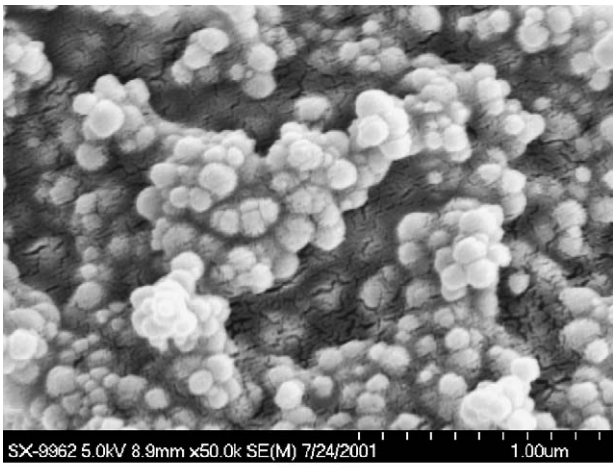

Fig. 5. SEM micrographs of BT6 ($BaCl_2$ and $Ti(OC_2H_5)_4$) and BT7 ($Ba(OAc)_2$ and $TiCl_4$) powders prepared by ACS process.

parameters, such as temperature, time, Ba/Ti ratio and pH were the same as those of BT2. No peak splitting of (2 0 0) and (0 0 2) at around $2\theta = 44.95^\circ$ in XRD indicating BT6 and BT7 are in cubic phase. The crystallite sizes of BT6 and BT7 are 50 ± 2 nm and 53 ± 2 nm, respectively, similar to BT2.

The morphology of BT6 from $Ti(OR)_4$ and $BaCl_2$ and BT7 from $TiCl_4$ and $Ba(OAc)_2$ shown in Fig. 5 is different from BT2 in Fig. 2b. Both BT6 and BT7 particles are spherical, but more particle agglomeration in BT6 and in BT7, which exhibits a broad particle size distribution from 120 to 200 nm. DLS data show that the mean particle size of BT6 is 207 ± 23 nm, and 164 ± 38 nm for BT7, little larger than BT2.

Based on the above results, it can be concluded that the morphology of $BaTiO_3$ particles is affected slightly by the anions in the precursors. In comparing the precursors for BT6 and BT7, BT7 has acetate chelating group from $Ba(OAc)_2$, and the greater complexation of the acetate anions is believed to result in the smaller particle size of BT7. Similar results have also been reported by other researchers.[22,58]

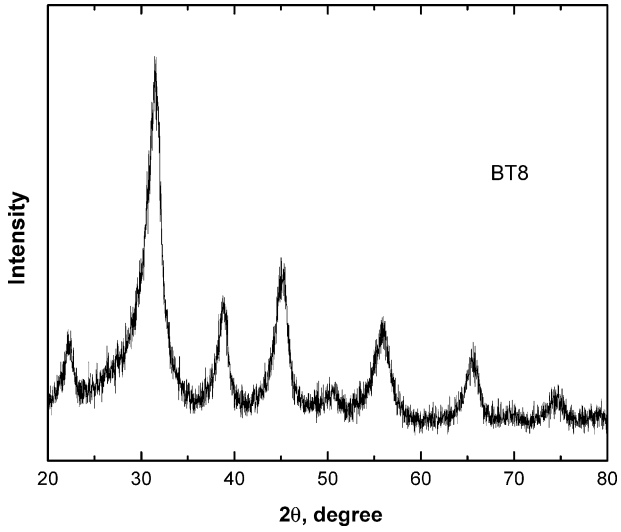

Fig. 6. RTXRD pattern of BT8 (with TMAH) powder shows significant peak broadening.

3.5. Effect of mineralizer

The precursor gel for ACS process was obtained by chemically precipitating staring chemicals in a highly basic solution. Could the inorganic base KOH be replaced by another organic base, and in turn some property changes in the final products? In this research, tetramethylammonium hydroxide (TMAH) was used in place of KOH, to adjust the pH of the precursor solution to 14.0 and the resulting $BaTiO_3$ was labeled as BT8. RTXRD pattern, as shown Fig. 6, of the BT8 powders shows cubic phase, similar to the other previous results. However, significant peak broadening is observed, indicating either poor crystallinity or very small crystallite size less than 10 nm.

All BT8 particles are spherical with a softer appearance (Fig. 8a) as compared to those particles prepared with KOH. Moreover, each individual BT8 particle is found to comprise of many much smaller particles at a closer observation by TEM in Fig. 7b. Thus, the broad RTXRD pattern in Fig. 7 must be caused by the crystallite size less than 10 nm.

Similar to KOH as a strong base, TMAH undergoes complete dissociation in water.

$$N(CH_3)_4{}^+OH^- \rightarrow N(CH_3)_4{}^+ + OH^- \quad (2)$$

While the precursor gels are forming via chemical precipitation, some cations are adsorbed onto the cluster of precursor gels. Obviously $N(CH_3)_4{}^+$ ion is much larger than K^+ and can stabilize and inhibit further growth of the nuclei. However, since the nuclei are small (<10 nm by XRD), they tend to aggregate into larger particles. The high weight loss (13.2 wt.%) at 800 °C in TGA curve (not shown in this paper) confirms that there is large amount of organic species and water in BT8 powders. DLS results show the particle size of BT8 is 146 ± 16 nm, indicating the aggregates of tiny crystals are difficult to break.

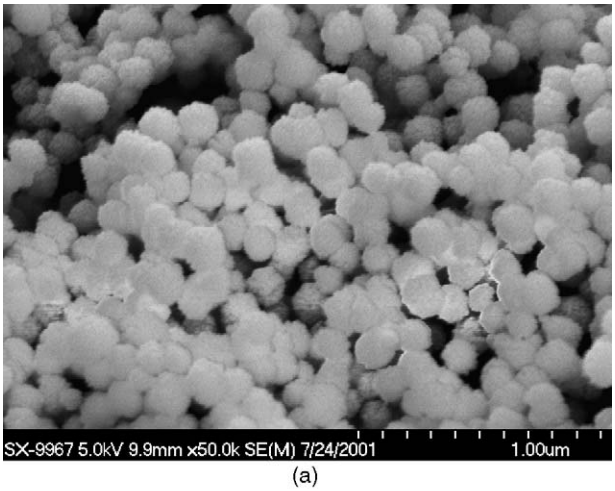

Fig. 7. SEM (a) and TEM (b) micrographs of BT8 powders.

3.6. Effect of polymer additive

A $BaTiO_3$ sample labeled as BT9 has been made in the presence of ammonium polyacrylate (APA) of a mean molecular weight of 6000 g/mol at a concentration of 0.002 g/ml. All other experimental parameters, such as the pH, Ba/Ti, and reaction time were similar to BT2.

No notable differences between the RTXRD patterns of BT2 and BT9 powders having cubic phase were observed. The crystallite size of BT9 calculated by the FWHM of (2 0 0) peak is 46.7 ± 1.4 nm. Near spherical $BaTiO_3$ powders are observed in the SEM micrograph (Fig. 8). Moreover, BT9 particles are smaller than those of BT2, indicating that the particle growth is somewhat inhibited by the adsorbed APA molecule.

The DLS results in Fig. 9 also indicate that the BT9 powders possess re-dispersibility. The particle size of as-prepared

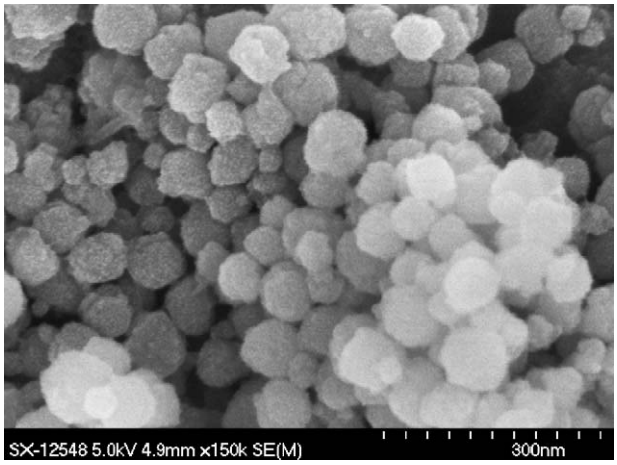

Fig. 8. SEM micrograph of BT9 powders prepared with APA.

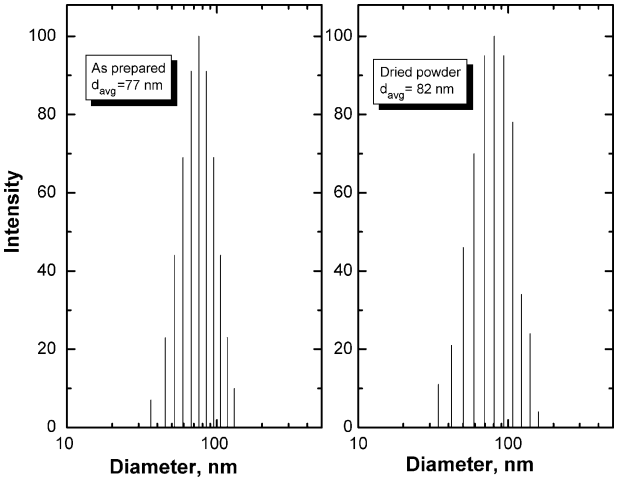

Fig. 9. Particle size distribution of BT9, as-prepared (left) and re-dispersed after air drying (right).

(wet powder) and re-dispersed (dried powder) in water are measured by DLS technique. The results show that the particle size of re-dispersed BT9 powders is almost the same as the BT9 particles before drying; indicating that introducing polymer dispersant during particle synthesis can result in re-dispersible powders.

4. Conclusions

Ambient condition sol (ACS) process produces nanocrystalline cubic phase BaTiO3 particles. The ACS process involves chemical precipitation of a Ba^{2+}-Tinania gel followed by peptization of the gel by refluxing in an aqueous medium. Among the processing variables, higher initial pH and Ba/Ti molar ratio led to smaller crystallite size of $BaTiO_3$ powders. Organic mineralizer, tetramethylammonium hydroxide (TMAH), can adsorb on the $BaTiO_3$ nuclei and further inhibit primary particle/crystal growth. The morphology of the

$BaTiO_3$ powders was affected slightly by the anion groups in the precursor species. Addition of a polymer dispersant, such as APA, during $BaTiO_3$ synthesis led to a smaller particle size and increased re-dispersibility of the particles in water.

Acknowledgements

This work is sponsored by the Division of Materials Science, Office of Basic Energy Sciences, of the U.S. Department of Energy, and partially supported by National Science Foundation with Grant Number DMR-9731769. Research is also sponsored in part by the Assistant Secretary for Energy Efficiency and Renewable Energy, Office of Transportation Technologies, as part of the High Temperature Materials Laboratory User Program, Oak Ridge National Laboratory, managed by UT-Battelle, LLC, for the U.S. Dept. of Energy under contract DE-AC05-00OR22725. Any opinions, findings, and conclusions, or recommendations expressed here are those of authors and do not necessarily reflect the views of the sponsors.

References

1. Dawson, W. J., Preston, J. C. and Swartz, S. L., Processing issues of hydrothermal synthesis of fine dielectric powders. In *Ceramics Trans., Vol 22, Ceramic Powder Science IV*, ed. S. Hirano, G. L. Messing and H. Hausner. Am Ceram Soc, Columbus (OH), 1991, p. 27.
2. Stockenhuber, M., Mayer, H. and Lercher, J. A., *J. Am. Ceram. Soc.*, 1993, **76**(5), 1185.
3. Zhao, L., Chien, A. T., Lange, F. F. and Speck, J. S., *J. Mater. Res.*, 1996, **11**(6), 1325.
4. Her, Y. S. and Matijevic, E., *J. Mater. Res.*, 1995, **10**(12), 3106.
5. Dutta, P. K. and Gregg, J. R., *Chem. Mater.*, 1992, **4**, 843.
6. Bagwell, R. B., Sindel, J. and Sigmund, W., *J. Mater. Res.*, 1999, **14**(5), 1844.
7. Maclaren, I. and Ponton, C. B., *J. Eur. Ceram. Soc.*, 2000, **20**, 1267.
8. Vivekanandan, R., Philip, S. and Kutty, T. R. N., *Mater. Res. Bull.*, 1986, **22**(1), 99.
9. Moon, J., Kerchner, J. A., Krarup, H. and Adair, J. H., *J. Mater. Res.*, 1999, **14**(2), 425.
10. Venigalla, S., Clancy, D. J., Miller, D. V., Kerchner, J. A. and Constantino, S. A., *Am. Cerm. Soc. Bull.*, 1999, **78**(10), 51.
11. Nowotny, J. and Rekas, M., *Electronic Ceramic Materials*. Trans Tech, Zurich, Switzerland, 1992, p. 1.
12. Bauger, A., Mutin, J. C. and Niepce, J. C., *J. Mater. Sci.*, 1983, **18**, 3041.
13. Chu, M. S. H. and Rae, A. M., *Am. Ceram. Soc. Bull.*, 1995, **74**, 69.
14. Phule, P. P. and Risbud, S. H., *J. Mater. Sci.*, 1990, **25**, 1169.
15. Lopez, M. C. B., Fourlaris, G., Rand, B. and Riley, F. L., *J. Am. Ceram. Soc.*, 1999, **82**, 1777.
16. Wilson, J. M., *Am. Ceram. Soc. Bull.*, 1995, **74**, 106.
17. Hertl, W., *J. Am. Ceram. Soc.*, 1988, **71**, 879.
18. Vivekanandan, R. and Kutty, T. R. N., *Powder Technol.*, 1989, **57**, 181.
19. Hennings, D., Rosenstein, G. and Schreinemacher, H., *J. Eur. Ceram. Soc.*, 1991, **8**, 107.
20. Hennings, D. and Schreinemacher, S., *J. Eur. Ceram. Soc.*, 1992, **9**, 41.
21. Dutta, P. K., Asiaie, R., Akbar, S. A. and Zhu, W. D., *Chem. Mater.*, 1994, **6**, 1542.
22. Xia, C. T., Shi, E. W., Zhong, W. Z and Guo, J. K., *J. Eur. Ceram. Soc.*, 1995, **15**, 1171.
23. Eckert Jr., J. O., Houst, C. C. H., Gersten, B. L., Lencka, M. M. and Riman, R. E., *J. Am. Ceram. Soc.*, 1996, **79**, 2929.
24. Asiaie, R., Zhu, W. D., Akbar, S. A. and Dutta, P. K., *Chem. Mater.*, 1996, **8**, 226.
25. Shi, E. W., Xia, C. T., Zhong, W. Z., Wang, B. G. and Feng, C. D., *J. Am. Ceram. Soc.*, 1997, **80**, 1567.
26. Zhu, W. D., Akbar, S. A., Asiaie, R. and Dutta, P. K., *Jpn. Appl. Phys.*, 1997, **36**, 214.
27. Hennings, D., Metzmacher, C. and Schreinemacher, B. C., *J. Am. Ceram. Soc.*, 2001, **84**, 179.
28. Urek, S. and Drofenik, M., *J. Eur. Ceram. Soc.*, 1998, **18**, 279.
29. Pinceloup, P., Courtois, C., Leriche, A. and Thierry, B., *J. Am. Ceram. Soc.*, 1999, **82**, 3049.
30. Clark, I. J., Takeuchi, T., Ohtori, N. and Sinclair, D., *J. Mater. Chem.*, 1999, **9**, 83.
31. Lu, S. W., Lee, B. I., Wang, Z. L. and Samuels, W. D., *J. Crystal Growth*, 2000, **219**, 269.
32. Hu, M. Z., Miller, G. A., Payzant, E. A. and Rawn, C. J., *J. Mater. Sci.*, 2000, **35**, 2927.
33. Hu, M. Z., Kurian, V., Payzant, E. A., Rawn, C. J. and Hunt, R. D., *Powder Technol.*, 2000, **110**, 2.
34. Xu, H. R., Gao, L. and Guo, J. K., *J. Eur. Ceram. Soc.*, 2002, **22**, 1163.
35. Ciftci, E., Rahaman, M. N. and Shumsky, M., *J. Mater. Sci.*, 2001, **36**, 4875.
36. Shimooka, H. and Kuwabara, M., *J. Am. Ceram. Soc.*, 1996, **79**, 2983–2985.
37. Frey, M. H. and Payne, D. H., *Chem. Mater.*, 1995, **7**, 123.
38. Matsuda, H., Kuwabara, M., Yamada, K., Shimooka, H. and Takahashi, S., *J. Am. Ceram. Soc.*, 1998, **81**, 3010.
39. Lee, B. I. and Zhang, J. P., *Thin Solid Films*, 2001, **388**, 107.
40. Matsuda, H., Kobayashi, N., Kobayashi, T., Miyazawa, K. and Kuwabara, M., *J. Non-Cryst. Solids*, 2000, **271**, 162.
41. Beck, H. P., Eiser, W. and Haberkorn, R., *J. Eur. Ceram. Soc.*, 2001, **21**, 687.
42. Nanni, P., Leoni, M., Buscaglia, V. and Alipandi, G., *J. Eur. Ceram. Soc.*, 1996, **14**, 85.
43. Leoni, M., Viviani, M., Nanni, P. and Buscaglia, V., *J. Mater. Sci. Lett.*, 1996, **15**, 1302.
44. Viviani, M., Lemaitre, J., Buscaglia, M. T. and Nanni, P., *J. Eur. Ceram. Soc.*, 2000, **20**, 315.
45. Wada, S., Chikamori, H., Noma, T. and Suzuki, T., *J. Mater. Sci.*, 2000, **35**, 4857.
46. Wada, S., Tsurumi, T., Chikamori, H., Noma, T. and Suzuki, T., *J. Crystal Growth*, 2001, **229**, 433.
47. Anuradha, T. V., Ranganathan, S., Mimani, T. and Patil, K. C., *Scripta Mater.*, 2001, **44**, 2237.
48. Gallagher, P. K. and Schrey, F., *J. Am. Ceram. Soc.*, 1963, **46**, 567.
49. Ma, Y., Vileno, E., Suib, S. L. and Dutta, P. K., *Chem. Mater.*, 1997, **9**, 3023.
50. Wang, J., Fang, J., Ng, S. C., Gan, L. M., Chew, C. H., Wang, X. B. *et al.*, *J. Am. Ceram. Soc.*, 1999, **82**, 873.
51. Busca, G., Buscaglia, V., Leoni, M. and Nanni, P., *Chem. Mater.*, 1994, **6**, 955.
52. Demazeau, G., *J. Mater. Chem.*, 1999, **9**, 15.
53. Chen, D. R. and Jiao, X. L., *J. Am. Ceram. Soc.*, 2000, **83**, 2637.

54. O'Brien, S., Brus, L. and Murry, C. B., *J. Am. Ceram. Soc.*, 2001, **123**, 12085.
55. Wang, X., Lee, B. I., Hu, M., Payzant, E. A. and Blom, D. A., *J. Mater. Sci. Lett.*, 2003, **22**, 557.
56. Wang, X., Lee, B. I., Hu, M., Payzant, E. A. and Blom, D. A., *J. Mater. Sci. Mater. Electron.*, 2003, **14**, 495.
57. Lencka, M. M. and Riman, E., *Chem. Mater.*, 1993, **5**, 61.
58. Wu, M., Xu, R. and Feng, S. H., *J. Mater. Sci.*, 1997, **31**, 6201.
59. Devaraju, N.G., Wang, X., Lee, B.I., Viviani, M. and Nanni, P., Tailoring size of BaTiO3 nanocrystals via ambient conditions sol process, *J. Mater. Sci*., submitted for publication.